Development 128, 4415-4424 (2001)
Printed in Great Britain © The Company of Biologists Limited 2001
DEV1720

The upstream ectoderm enhancer in *Pax6* has an important role in lens induction

Patricia V. Dimanlig[1], Sonya C. Faber[1], Woytek Auerbach[1,2], Helen P. Makarenkova[1] and Richard A. Lang[1,*,‡]

[1]Developmental Genetics Program, Skirball Institute for Biomolecular Medicine, New York University School of Medicine, 540 First Avenue, New York, NY 10016, USA
[2]Howard Hughes Medical Institute, Cell Biology Department, New York University School of Medicine, 540 First Avenue, New York, NY 10016, USA
*Present address: Children's Hospital Research Foundation, Developmental Biology Division, Department of Ophthalmology, 3333 Burnet Avenue, Cincinnati, OH45229-3039, USA
‡Author for correspondence (e-mail: richard.lang@chmcc.org)

Accepted 24 July 2001

SUMMARY

The *Pax6* gene has a central role in development of the eye. We show, through targeted deletion in the mouse, that an ectoderm enhancer in the *Pax6* gene is required for normal lens formation. Ectoderm enhancer-deficient embryos exhibit distinctive defects at every stage of lens development. These include a thinner lens placode, reduced placodal cell proliferation, and a small lens pit and lens vesicle. In addition, the lens vesicle fails to separate from the surface ectoderm and the maturing lens is smaller and shows a delay in fiber cell differentiation. Interestingly, deletion of the ectoderm enhancer does not eliminate Pax6 production in the lens placode but results in a diminished level that, in central sections, is apparent primarily on the nasal side. This argues that *Pax6* expression in the lens placode is controlled by the ectoderm enhancer and at least one other transcriptional control element. It also suggests that *Pax6* enhancers active in the lens placode drive expression in distinct subdomains, an assertion that is supported by the expression pattern of a *lacZ* reporter transgene driven by the ectoderm enhancer. Interestingly, deletion of the ectoderm enhancer causes loss of expression of *Foxe3*, a transcription factor gene mutated in the *dysgenetic lens* mouse. When combined, these data and previously published work allow us to assemble a more complete genetic pathway describing lens induction. This pathway features (1) a pre-placodal phase of *Pax6* expression that is required for the activity of multiple, downstream *Pax6* enhancers; (2) a later, placodal phase of *Pax6* expression regulated by multiple enhancers; and (3) the *Foxe3* gene in a downstream position. This pathway forms a basis for future analysis of lens induction mechanism.

Key words: Lens induction, Lens development, Pax6, Transcriptional enhancer, Foxe3, Dysgenetic lens, Mouse

INTRODUCTION

Pax6 is a homeobox transcription factor acknowledged to have a critical, evolutionarily conserved role in eye development. This is highlighted by loss-of-function mutations in *Drosophila* (Quiring et al., 1994), mouse (Hogan et al., 1986) and human (Bickmore and Hastie, 1989), in which eye development is affected. In humans, these conditions include the autosomal dominant aniridia (Ton et al., 1991) and Peters' anomaly (Hanson et al., 1994). In mice, heterozygous *Pax6* mutations result in the phenotype *Small eye* (*Sey*) (Hill et al., 1991). Mouse embryos homozygous for the *Sey* mutations show anophthalmia and disrupted nasal development and die perinatally due to inability to breathe (Hogan et al., 1986; Hill et al., 1991). In *Drosophila*, there are two *Pax6* homologs called *eyeless* (Quiring et al., 1994) and *twin-of-eyeless* (Czerny et al., 1999), and either can induce the formation of ectopic eyes when expressed in imaginal discs (Halder et al., 1995). Gain-of-function experiments in *Xenopus* indicate that in vertebrates too, *Pax6* is sufficient for eye development in the context of the whole embryo (Chow et al., 1999).

Several experiments indicate that *Pax6* is essential for the formation of the lens. Aggregation of cells from wild-type and *Sey* embryos results in chimeric mice in which *Sey* mutant cells are excluded from the lens placode at embryonic day (E) 9.5 (Collinson et al., 2000) and from the maturing lens at E12.5 (Quinn et al., 1996). Additionally, tissue recombination experiments demonstrate that lens formation is prevented when the *Sey* mutation is present in the presumptive lens ectoderm (Fujiwara et al., 1994). These findings were corroborated by recent work in which the deletion of *Pax6* in the prospective lens ectoderm by conditional gene targeting techniques resulted in lack of lens formation (Ashery-Padan et al., 2000).

Pax6 expression is detected in a number of regions of the developing mouse central nervous system, including the presumptive retina from the headfold stage onwards (Walther

and Gruss, 1991; Stoykova and Gruss, 1994; Grindley et al., 1995). In addition, *Pax6* expression is found in a large area of head surface ectoderm. The broad *Pax6* expression domain in the head ectoderm is first observed at E8.0 and becomes progressively restricted to the developing lens and nasal placodes. Assessment of *Pax6* mRNA expression patterns in wild-type and homozygous *Pax6*$^{Sey\text{-}1Neu/Sey\text{-}1Neu}$ mutant mice illustrates that *Pax6* expression in the surface ectoderm can be divided into at least two stages (Grindley et al., 1995). The first stage corresponds to *Pax6* in the surface ectoderm before close contact with the optic vesicle. The second stage occurs after contact, and correlates with the formation of the lens placode. The observation that *Pax6* gene expression in the lens lineage ceases after E9.5 in the *Pax6*$^{Sey\text{-}1Neu/Sey\text{-}1Neu}$ mouse indicates that the second phase of *Pax6* transcription is dependent on the first (Grindley et al., 1995). Thus, functional Pax6 in the surface ectoderm is required for continued placodal *Pax6* expression and subsequent lens development.

Pax6 expression in the lens lineage is, at least in part, regulated by a highly conserved transcriptional enhancer that is active in the surface ectoderm adjacent to the optic vesicle as well as the lens placode beginning at E8.75 (Williams et al., 1998). This ectoderm enhancer (EE) is also active in derivatives of the lens placode that include the presumptive corneal epithelium, conjunctival epithelium and lacrimal gland epithelium (Williams et al., 1998; Kammandel et al., 1999; Makarenkova et al., 2000). The EE is located approximately 4 kb upstream of the start site of transcription of the first promoter in the mouse *Pax6* gene (Williams et al., 1998) and offers both a useful tool to direct transgene expression to the lens lineage, and a starting reagent with which to identify factors that regulate *Pax6* expression.

As a first step in studying the function of this enhancer, we have used a loss-of-function strategy and deleted the enhancer through targeted mutagenesis in the mouse. *Pax6* ectoderm enhancer-null embryos still execute lens development but exhibit a range of lens defects. These include a reduction in lens placode thickness and proliferation rate, smaller lenses, delayed primary fiber cell differentiation and a persistent connection between the lens and surface ectoderm. Consistent with deletion of a transcriptional enhancer, we find diminished levels of Pax6 in the lens placode. Interestingly, reductions in Pax6 levels and ectodermal thickness within the lens placode occur primarily on the nasal side, suggesting the existence of *Pax6* expression subdomains under the regulation of distinct enhancers. The existence of a second *Pax6* placodal enhancer is also consistent with the observation that lens development proceeds in the enhancer null mice, albeit abnormally. Loss of expression of *Foxe3*, a gene required for certain aspects of lens development (Blixt et al., 2000; Brownell, et al., 2000), allows us to more completely define the genetic relationships within the lens induction pathway.

MATERIALS AND METHODS

Gene targeting

Standard techniques of targeted mutagenesis and embryonic stem (ES) cell manipulation were used to generate a deletion of the *Pax6* EE in the mouse. A 6.5 kb *Sac*II-*Aat*II fragment containing the *Pax6* EE was isolated from a mouse 129/SvJ ES cell genomic BAC library (Genome Systems). This fragment was sublconed into the double-selection gene replacement vector pKS*loxP*NT (containing a *loxP*-flanked PGK*neo* cassette and the Herpes Simplex Virus *tk* gene (Hanks et al., 1995)), replacing the floxed *neo* cassette. A 1.7 kb *Eco*RI fragment was removed from this construct and replaced with the *Eco*RI-digested product of a two-step nested polymerase chain reaction (PCR), using the 6.5 kb *Sac*II-*Aat*II fragment as the initial template. The primers used for step 1 were: Primer 1F (5′-CCATAGAGTTTTCATCCTAGAT-3′) and Primer 2R (5′-TTTGGCCGGCCGTCATTTAATGGTTAATTAAGGGAAAGGATGGCTTAGTAATTTAAAC-3′) for reaction 1; and Primer 3F (5′-CCCTTAATTAACCATTTAAATGACGGCCGGCCAAAAAGACA-GTGGAATGTTCTTGAAT-3′) and Primer 4R (5′-TTCTTTCAAATCAAAATGGGA GG-3′) for reaction 2. For step 2, Primer 1F and Primer 4R (which both contained *Eco*RI sites) were used to amplify the final PCR product, using the combined products of reactions 1 and 2 as the templates. The resulting PCR product effectively removed the 341 bp ectoderm enhancer and introduced new *Pac*I, *Swa*I and *Fse*I restriction sites in its place. The floxed *neo* cassette was subsequently sublconed into the new *Swa*I site. The completed targeting vector contained 2.7 kb and 3.6 kb 5′ and 3′ targeting arms, respectively, and was sequenced to verify the deletion and junctions. R1 ES cells were electroporated (Joyner, 1995) with the targeting construct linearized at *Kpn*I. Colonies that passed positive and negative selection were clonally isolated and screened by Southern blot analysis with both 5′ and 3′ probes. Blastocyst injection chimeras were crossed with Black Swiss animals to assess germline transmission. The floxed *neo* selection cassette was deleted by crossing with transgenic germline *Cre* recombinase mice (W. A., unpublished) that express *cre* recombinase in the germline. The resulting progeny were intercrossed to produce the stock used for the experiments described here. Genotyping was performed by PCR using genomic DNA obtained from mouse tails or embryonic yolk sacs. The primers used for PCR genotyping were: P1 (5′-AAGCACCCCAACCTCATTCTTTTCACCTCC-3′), P2 (5′-AGTTAGTTTGCTTTCCCCACTGAGAAAA-GCC-3′), and P3 (5′-GCCAAGTTCTAATTCCATCAGAAGCTGACTC-3′). The PCR conditions used were as follows: 35 cycles of 94°C for 15 seconds, 57°C for 30 seconds, 72°C for 30 seconds. The expected PCR fragment sizes are 469 bp for the wild-type allele, 205 bp for the targeted (+*neo*) allele, and 260 bp for the targeted (–*neo*) allele.

Histological analysis

Samples for routine histology were collected into cold phosphate-buffered saline (PBS) and fixed in phosphate-buffered 4% paraformaldehyde (PFA) or 10% neutral buffered formalin. The samples were dehydrated and embedded in paraffin, cut as 4 μm sections, and stained with Hematoxylin and Eosin.

For immunohistochemistry, 5 μm dewaxed paraffin sections and 20 μm cryosections were used. To ensure consistency of the section plane and angle of the eye for comparison of Pax6 immunofluorescence in wild-type and mutant embryos, we were rigorous about the orientation of the embryos at the embedding stage. Embryo heads were rested against the base of the embedding mold on the dorsal surface of the forebrain/midbrain. The section plane used for Pax6 immunofluoresence comparisons is shown by the broken line in Fig. 5B. The sections were blocked for 1 hour with blocking solution (10% normal serum/0.1% Triton X-100 in PBS), incubated for 2 hours with primary antibodies, washed with blocking solution, incubated for 40 minutes with secondary antibodies, washed with PBS and mounted with Gelmount. All incubations were performed at room temperature. Primary antibodies used were anti-α-crystallin and anti-β-crystallin at 1:500 dilution each (Zigler and Sidbury, 1976), and polyclonal anti-Pax6 (Covance) also at 1:500 dilution. Secondary antibodies were Alexa goat anti-rabbit IgG (Molecular Probes) used at a 1:500 dilution. Sections were counterstained with Hoechst 33258 to visualize nuclei. Images for all histological analysis were captured using a Zeiss Axiophot microscope and a Sony DKC 5000 digital camera. The green staining corresponds to Pax6 immunolabeling, while the yellow staining emphasizes areas with more intense labeling.

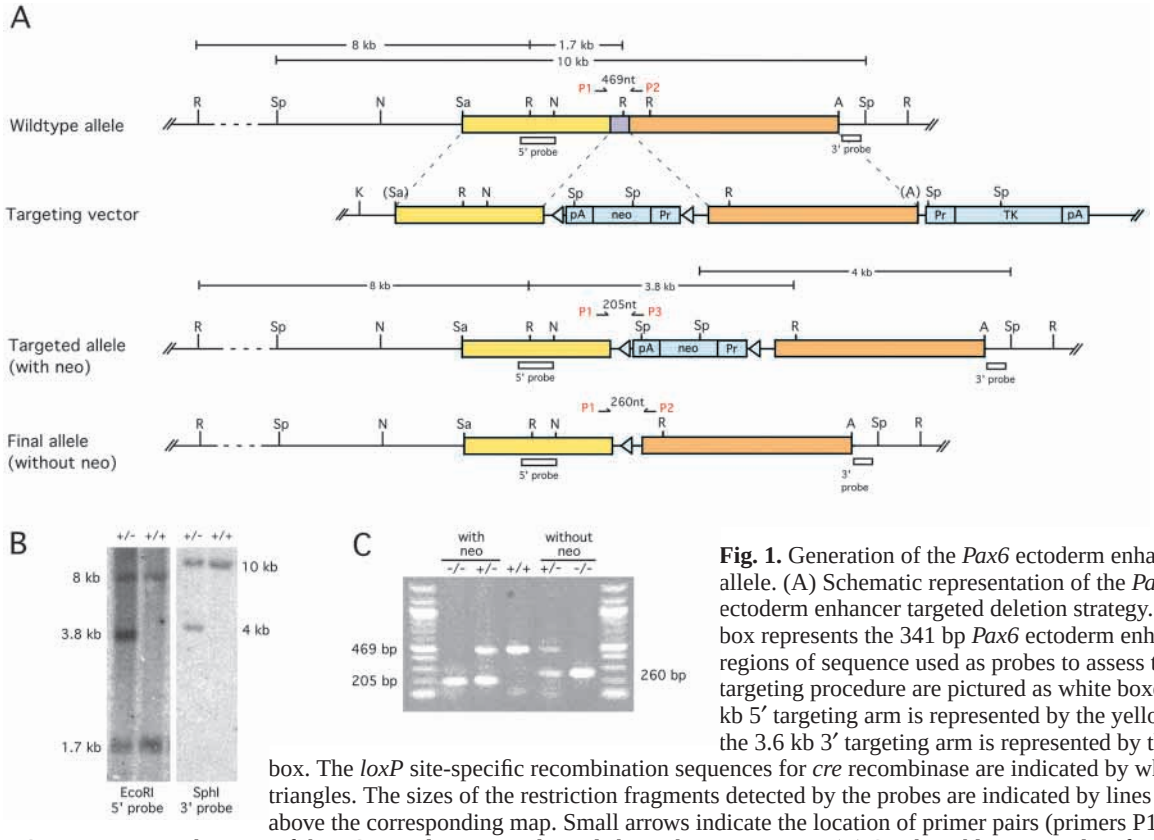

Fig. 1. Generation of the *Pax6* ectoderm enhancer null allele. (A) Schematic representation of the *Pax6* ectoderm enhancer targeted deletion strategy. The purple box represents the 341 bp *Pax6* ectoderm enhancer. The regions of sequence used as probes to assess the targeting procedure are pictured as white boxes. The 2.7 kb 5′ targeting arm is represented by the yellow box, and the 3.6 kb 3′ targeting arm is represented by the orange box. The *loxP* site-specific recombination sequences for *cre* recombinase are indicated by white triangles. The sizes of the restriction fragments detected by the probes are indicated by lines located above the corresponding map. Small arrows indicate the location of primer pairs (primers P1, P2 and P3) used for PCR genotyping. The sizes of the PCR products are indicated above the primer pairs. (B) Southern blotting to identify wild-type (+/+) and targeted (where +/– designates +/*neoΔEE*) ES cell-line genomic DNA for *Eco*RI and *Sph*I restriction digests probed with the 5′ and 3′ probes, respectively. The fragment sizes are labeled next to the appropriate bands. (C) PCR genotyping of genomic DNA. The sizes of PCR products are indicated to the left and right of the gel panel. R, *Eco*RI; N, *Nco*I; Sa, *Sac*II; Sp, *Sph*I; A, *Aat*II; K, *Kpn*I; *neo*, neomycin phosphotransferase gene; *tk*, thymidine kinase gene; pA, polyadenylation signal; Pr, promoter.

BrdU analysis

Pregnant mice were injected intraperitoneally with 100 μg of 5-bromo-2′-deoxyuridine (BrdU) and 7 μg of 5-fluoro-2′-deoxyuridine dissolved in 0.007 M NaOH per gram body weight. Embryos were collected one hour after injection, fixed with 4% PFA and embedded in paraffin. 5 μm sections were cut and processed as described earlier (Takahashi et al., 1993). Sections were incubated with monoclonal anti-BrdU antibody (Harlan) at a 1:100 dilution for 2 hours at room temperature. The secondary antibody used was Alexa goat anti-rat IgG (Molecular Probes) at a 1:500 dilution. Sections were counterstained with Hoechst 33258 to visualize nuclei.

Whole-mount gene expression analysis

Whole-mount in situ hybridization was performed as described (Nieto et al., 1996). The *Foxe3* antisense probe was generated from a plasmid containing the 5′ end and 5′ UTR sequence of *Foxe3* (Brownell et al., 2000). Expression activity from the ectoderm enhancer was assessed using the *P6 5.0-lacZ* animals as previously described (Williams et al., 1998).

RESULTS

Generation of *Pax-6* ectoderm enhancer-deficient mice

In order to investigate the role of the *Pax6* EE in lens development, we deleted the defined 341 bp region (Williams et al., 1998) by homologous recombination in embryonic stem cells. The gene targeting strategy is shown in Fig. 1A. The targeted allele was detected in embryonic stem cells by Southern hybridization using 5′ internal and 3′ external probes (Fig. 1B). Genotyping of mice and confirmation of *neo* cassette excision was performed by PCR analysis (Fig. 1C). Removal of the *neo* cassette via *cre*-mediated homologous recombination results in a final allele in which a single *loxP* site has replaced the 341 bp EE element. This allele is referred to as $Pax6^{\Delta EE}$.

Pax6$^{\Delta EE/\Delta EE}$ embryos have abnormal early lens development

Adult heterozygous and homozygous mutant animals are viable and fertile, and show no gross abnormalities. However, both genotypes exhibit distinct phenotypes during the earliest stages of lens development. By E9.0 in wild-type embryos, the optic vesicle has extended from the diencephalon and has made contact with the surface ectoderm. The portion of the surface ectoderm which contacts the optic vesicle normally thickens to form the lens placode (Fig. 2A) and will later invaginate and separate from the surface ectoderm to become the lens vesicle. At E9.5 in the $Pax6^{+/\Delta EE}$ (Fig. 2B) and $Pax6^{\Delta EE/\Delta EE}$ (Fig. 2C) mutant embryos, the surface ectoderm directly apposed to the optic vesicle is markedly thinner in the nasal portion. This regional reduction in placodal thickness is quantified in experiments described below. By E10.5, the lens placode invaginates and forms the lens pit. The mutant lens pit is much

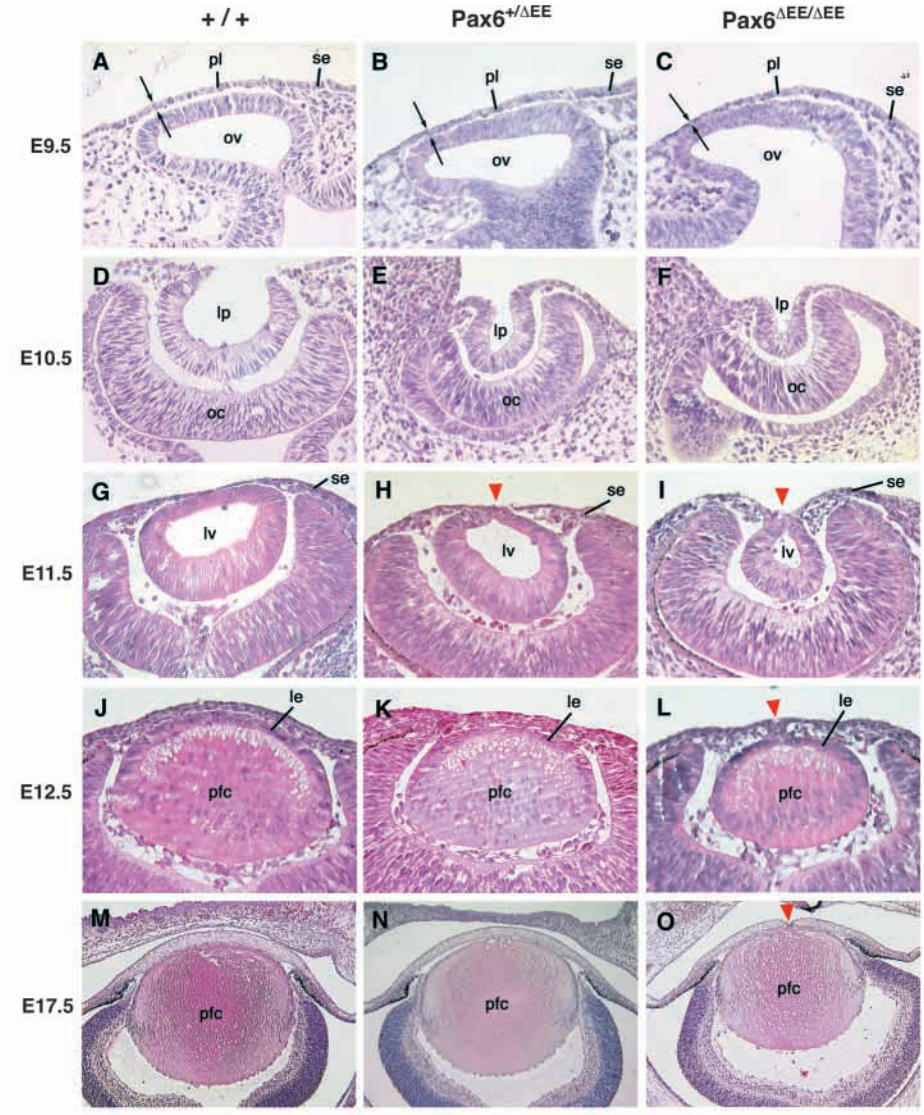

Fig. 2. Histological analysis of *Pax6*$^{\Delta EE/\Delta EE}$ mice. All panels show Hematoxylin and Eosin stained 4 μm paraffin sections. E9.5 eyes from WT (A), *Pax6*$^{+/\Delta EE}$ (B) and *Pax6*$^{\Delta EE/\Delta EE}$ (C) embryos. This shows the optic vesicle (ov) in close contact with the surface ectoderm (se) that in the wild-type is thickened in the region of the lens placode (pl). In *Pax6*$^{\Delta EE/\Delta EE}$ embryos, the nasal aspect of the placodal ectoderm is abnormally thin (arrow). E10.5 eyes from wild type (D), *Pax6*$^{+/\Delta EE}$ (E) and *Pax6*$^{\Delta EE/\Delta EE}$ (F) embryos. The optic cup (oc) and lens pit (lp) have formed through coordinated invagination of optic vesicle and lens placode. In *Pax6*$^{\Delta EE/\Delta EE}$ embryos, the lens pit and optic cup are small. *Pax6*$^{+/\Delta EE}$ embryos show an intermediate phenotype. E11.5 eyes from wild type (G), *Pax6*$^{+/\Delta EE}$ (H) and *Pax6*$^{\Delta EE/\Delta EE}$ (I) embryos. In the wild type, the lens vesicle (lv) has separated form the surface ectoderm (se). In the homozygous mutant, the lens vesicle is small and remains attached (red arrowhead). Heterozygotes have an intermediate phenotype (red arrowhead). E12.5 eyes from wild type (J), *Pax6*$^{+/\Delta EE}$ (K) and *Pax6*$^{\Delta EE/\Delta EE}$ (L) embryos. At this stage, primary fiber cells (pfc) have extended from the posterior lens vesicle towards the lens epithelium (le) in both wild type and mutant embryos, but the homozygous mutant lens is small with a persistent lens stalk (red arrowhead). The optic cup in *Pax6*$^{\Delta EE/\Delta EE}$ embryos is marginally smaller than in wild type. Again, heterozygotes have an intermediate phenotype. E17.5 eyes from wild type (M), *Pax6*$^{+/\Delta EE}$ (N) and *Pax6*$^{\Delta EE/\Delta EE}$ (O) embryos. In eyes of this stage, both primary and secondary fiber cells have differentiated in all genotypes. A smaller lens is apparent in homozygotes and a local invagination of the corneal epithelium (red arrowhead) indicates a persistent lens stalk. Morphologically, pseudostratification in the retina appears unaffected.

smaller in size compared with wild-type (compare Fig. 2D with 2F), and the heterozygous structure (Fig. 2E) is intermediate in size. By E11.5, the wild-type lens vesicle has formed and is completely separated from the surface ectoderm (Fig. 2G). By contrast, the *Pax6*$^{\Delta EE/\Delta EE}$ lens vesicle is still connected to the surface ectoderm and remains very small (Fig. 2I). Again, in the E11.5 heterozygous littermate (Fig. 2H), we see a less severe separation defect than in *Pax6*$^{\Delta EE/\Delta EE}$ animals. By E12.5, the posterior cells of the lens vesicle have differentiated into primary fiber cells and extend anteriorly towards the undifferentiated lens epithelium (Fig. 2J). In the *Pax6*$^{\Delta EE/\Delta EE}$ mutant embryos at E12.5, elongation of the posterior lens vesicle cells has occurred, despite the reduced lens size (Fig. 2L). The mutant lens epithelial layer remains attached to the surface ectoderm, the future corneal epithelium (Fig. 2L, arrowhead). By contrast, the heterozygous lenses of intermediate size are completely separated from the surface ectoderm and have appropriately elongated posterior lens vesicle cells (Fig. 2K). By E17.5, the difference in size between the wild-type (Fig. 2M), *Pax6*$^{+/\Delta EE}$ (Fig. 2N) and *Pax6*$^{\Delta EE/\Delta EE}$ (Fig. 2O) lenses is not as great as in earlier stages, but the lens stalk remains in the homozygous mutants (Fig. 2O, red arrowhead). This persistent focal connection between lens and cornea is similar to the defect observed in Peters' anomaly, a congenital disorder observed in some humans and mice mutant for *Pax6* (Hanson et al., 1994), and which is characterized by a central corneal opacity, sometimes owing to a persistent lens stalk (Peters, 1906; Stone et al., 1976).

Ectodermal thickness and proliferation are reduced in EE-deficient embryos

As shown (Fig. 2C), the nasal region of the prospective lens ectoderm of *Pax6*$^{\Delta EE/\Delta EE}$ embryos appears to be thinner than that of wild-type at E9.5. In order to better quantify and describe this observation, we defined five equally spaced points along the ectoderm directly opposite the optic vesicles of wild-type, heterozygous, and homozygous mutant embryos, with point 1 being the most nasal and point 5 the most temporal

(Fig. 3A,B). The plane of section used for these measurements is illustrated (Fig. 3C). The ectoderm thickness at each of these five points was measured in wild-type, heterozygous and homozygous mutant embryos, and plotted for comparison (Fig. 3D). We found significant differences between wild-type and *Pax6*$^{\Delta EE/\Delta EE}$ ectodermal thickness, with the greatest divergence in the nasal half of the ectoderm. Heterozygous mutants showed an intermediate level of placodal thickness between that of wild-type and homozygous mutant embryos.

In seeking an explanation for the diminished size of lens lineage structures observed in mutant embryos, we determined the proportion of proliferating cells in the prospective lens ectoderm at E9.5. The ectoderm directly opposite the optic vesicle was scored according to the number of BrdU-positive cells divided by the total cell number (Figs 3E,F). The percentage of BrdU-positive cells in the prospective lens ectoderm is significantly different (error bars do not overlap and $P<0.038$ using Student's *t*-test) between wild-type and homozygous embryos (Fig. 3G). Thus, the lower level of proliferation in *Pax6*$^{\Delta EE/\Delta EE}$ embryos may account for the smaller size of lens lineage structures. No increase in the appearance of apoptotic figures in the lens has been observed in *Pax6*$^{\Delta EE/\Delta EE}$ embryos.

Lens fiber cell differentiation is delayed in *Pax6*$^{\Delta EE/\Delta EE}$ embryos

To determine whether EE deletion affected differentiation in the lens lineage, we performed immunofluorescence detection of differentiation markers. Crystallins are abundant soluble lens proteins that exhibit developmentally and spatially regulated expression (McAvoy, 1978; Cvekl et al., 1995a; Cvekl et al., 1995b; Richardson et al., 1995; Cvekl and Piatigorsky, 1996) making them valuable markers for assessing the progress of lens fiber cell differentiation. α-crystallins are the earliest family to be expressed and are first detected at E10.5 in the invaginating lens pit. α-crystallin expression continues in both the anterior epithelium and differentiating fiber cells in the developing lens. β-crystallin expression begins after α-crystallin, but unlike α-crystallin, is expressed only in the differentiating lens fiber cells.

At E11.5, wild-type embryos stained for α-crystallin show expression in both the anterior and posterior cells of the lens vesicle (Fig. 4A). Heterozygous mutant lenses show normal α-crystallin expression (Fig. 4B). In homozygous littermates, however, α-crystallin is detected at slightly lower levels in both

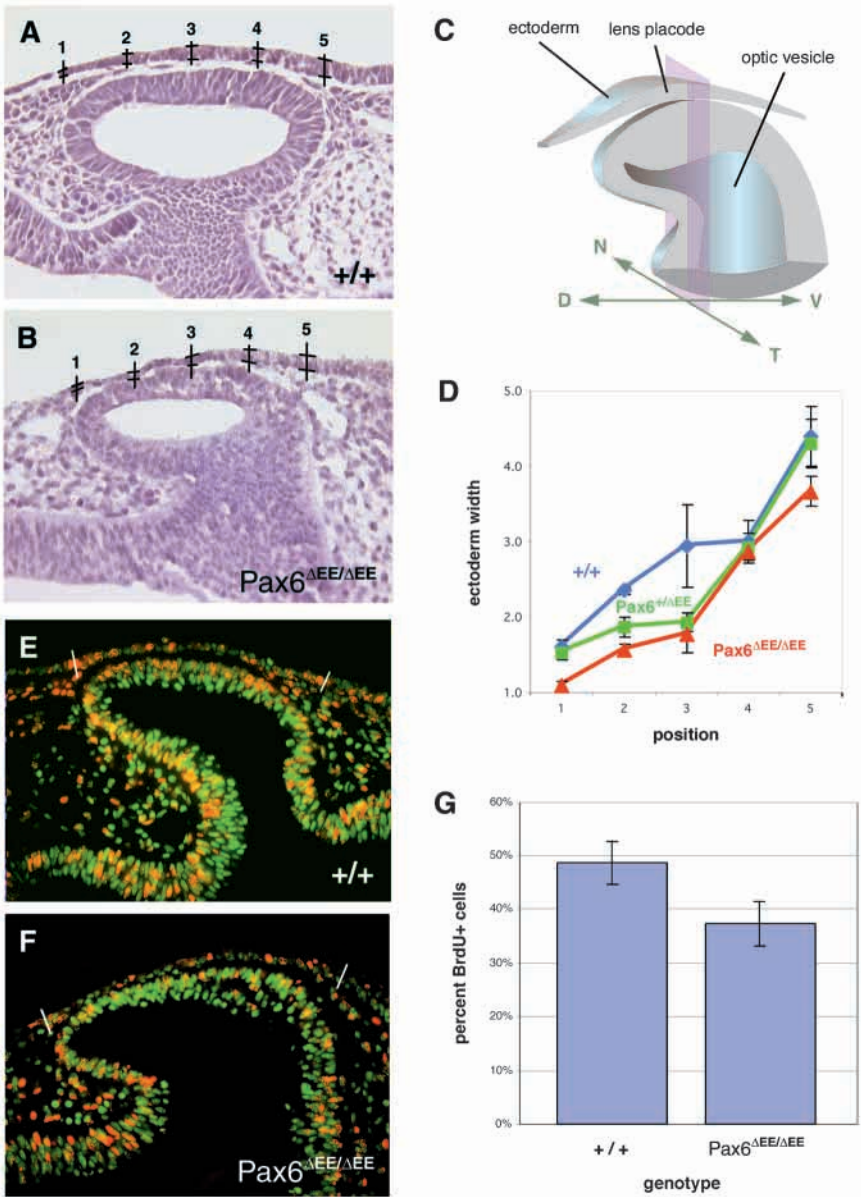

Fig. 3. Assessment of placodal thickness and proliferation in *Pax6*$^{\Delta EE/\Delta EE}$ mice. Wild-type (A) and *Pax6*$^{\Delta EE/\Delta EE}$ (B) eyes at E9.5 in paraffin section. The numbered vertical lines indicate the points in the surface ectoderm at which the thickness of the lens placode was measured. Position 1 is on the nasal side and position 5 temporal. This was performed using digitized images and an arbitrary unit system. (C) Schematic of an E9.5 eye showing the section plane (purple shading) used for placodal thickness measurements. D, V, N and T indicate the dorsal, ventral, nasal and temporal aspects, respectively. (D) Graph showing, in arbitrary units, a comparison of placodal thickness in wild type (blue) *Pax6*$^{+/\Delta EE}$ (green) and *Pax6*$^{\Delta EE/\Delta EE}$ (red) embryos. This indicates that in approximately the nasal half of the lens placode, the *Pax6*$^{\Delta EE/\Delta EE}$ placode is thinner than in wild type. The difference is greatest in the central placode and minimal in the temporal domain. *Pax6*$^{+/\Delta EE}$ embryos have an intermediate phenotype. Vertical bars represent standard errors. Wild-type (E) and *Pax6*$^{\Delta EE/\Delta EE}$ eyes (F) at E9.5 in paraffin section stained with Hoechst 33258 to indicate nuclei (green labeling) and with anti-BrdU detection reagents (red labeling). Only the green component of the blue Hoechst signal has been included in these images for ease of visualization. The percentage of BrdU-positive cells within the lens placode (white lines) was determined and presented in a histogram (G) comparing wild-type and *Pax6*$^{\Delta EE/\Delta EE}$ embryos. This indicated that the level of proliferation was reduced in the *Pax6*$^{\Delta EE/\Delta EE}$ lens placode. Vertical bars represent standard errors.

anterior and posterior cells of the smaller, attached lens (Fig. 4C). At E12.5 α-crystallin is also present in both anterior epithelium and fiber cells of the developing lens in wild-type animals, but by this time, the primary fiber cells have completed their extension towards the anterior epithelium (Fig. 4D). α-crystallin expression in heterozygous animals is comparable with wild-type (Fig. 4E). In *Pax6*$^{\Delta EE/\Delta EE}$ embryos, however, extension of the primary fiber cells is incomplete and there appear to be fewer labeled cells (Fig. 4F). In contrast to α-crystallin, β-crystallin expression appears to be more affected by absence of the *Pax6* enhancer. At E11.5, expression of β-crystallin in wild-type and heterozygous embryos is observed in the posterior cells of the lens vesicle (Figs 4G,H). In homozygous mutant littermates, β-crystallin expression is greatly downregulated in these cells (Fig. 4I). At E12.5, β-crystallin expression in wild-type and heterozygous lenses is found along the entire length of the fully elongated lens fiber cells (Figs 4J,K). However, in *Pax6*$^{\Delta EE/\Delta EE}$ embryos, β-crystallin expression is at a lower level in fewer cells (Fig. 4L). These data indicate a delay in the onset of fiber cell differentiation in *Pax6*$^{\Delta EE/\Delta EE}$ embryos.

EE deletion results in reduced levels of Pax6 and undetectable *Foxe3* expression

Pax6 expression in the head surface ectoderm is first observed in a broad domain at E8.0, and becomes progressively restricted to the developing lens and nasal placodes (Grindley et al., 1995). To gain a better understanding of the progression and extent of expression mediated by the EE at the earliest stages of lens development, we examined reporter transgene expression in *P6 5.0-lacZ* transgenic embryos where *lacZ* expression is driven by the ectoderm enhancer (Williams et al., 1998). *lacZ* expression is first observed at approximately E8.75 in a teardrop-shaped region of surface ectoderm that overlies the optic vesicle (Fig. 5A). By E9.5 expression is most intense in a crescent-shaped region that corresponds to the nasoventral lens placode (Fig. 5B,C).

To analyze the effect of EE deletion on the expression of *Pax6* in the surface ectoderm, we performed Pax6 immunolabeling on E9.5 cryosections from wild-type and homozygous mutant embryos. Compared with wild type (Fig. 5D), homozygous mutant embryos (Fig. 5E) show much diminished Pax6 levels in the nasal aspect of the surface ectoderm (this is emphasized by comparing levels of immunoreactivity on the nasal side (arrowheads) of the sections shown in Figs 5D,E). Interestingly, the area of greatest decrease in Pax6 levels in *Pax6*$^{\Delta EE/\Delta EE}$ embryos corresponds to the region of greatest *P6 5.0-lacz* reporter expression (Fig. 5C) and reduced ectodermal thickness (Fig. 3). Deletion of the *Pax6* EE therefore results in lower levels of Pax6 protein throughout the presumptive lens ectoderm, with the greatest decrease found nasally. At later stages of lens development, there were no obvious changes in the level or pattern of Pax6 immunoreactivity (Fig. 5F,G and data not shown). The morphological defects apparent in *Pax6*$^{\Delta EE/\Delta EE}$ embryos precluded a meaningful comparison in the central region of the lens epithelium.

We noted that the phenotype in *Pax6*$^{\Delta EE/\Delta EE}$ mice was in many respects similar to that observed in the *dysgenetic lens* (*dyl*) mouse (Blixt et al., 2000; Brownell et al., 2000). Both mutants have persistent lens stalks, as well as defects in lens proliferation and lens fiber cell differentiation. The *dyl* phenotype is a result of a mutation in the forkhead transcription factor *Foxe3* (Blixt et al., 2000; Brownell et al., 2000). *Foxe3*

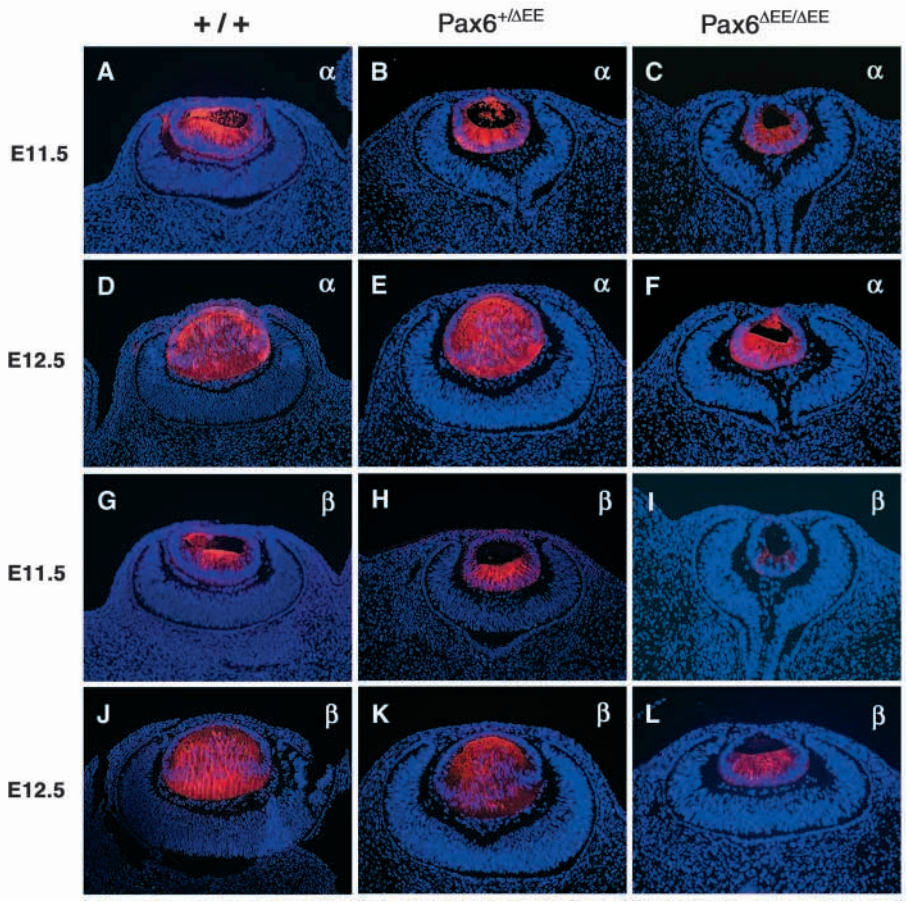

Fig. 4. Expression and distribution of differentiation markers in *Pax6*$^{\Delta EE/\Delta EE}$ mice. All panels show fluorescently labeled 4 μm paraffin sections counterstained with Hoechst 33258 to indicate nuclei (blue labeling). E11.5 eyes from wild-type (A), *Pax6*$^{+/\Delta EE}$ (B) and *Pax6*$^{\Delta EE/\Delta EE}$ (C) embryos labeled with anti-α-crystallin antibodies. *Pax6*$^{\Delta EE/\Delta EE}$ embryos show reduced per cell labeling and a smaller number of positive cells in the posterior lens vesicle. α-crystallin labeling at E12.5 of wild type (D), *Pax6*$^{+/\Delta EE}$ (E) and *Pax6*$^{\Delta EE/\Delta EE}$ (F) embryos emphasizes that there are fewer positive cells in the lens of the homozygous mutant. E11.5 eyes from wild-type (G), *Pax6*$^{+/\Delta EE}$ (H) and *Pax6*$^{\Delta EE/\Delta EE}$ (I) embryos labeled with anti-β-crystallin antibodies. *Pax6*$^{\Delta EE/\Delta EE}$ embryos show a reduced level of labeling on a per cell basis and fewer positive cells in the posterior lens vesicle. This indicates a suppression of fiber cell differentiation consistent with morphological findings. This observation is emphasized in comparing wild type (J), *Pax6*$^{+/\Delta EE}$ (K) and *Pax6*$^{\Delta EE/\Delta EE}$ (L) E12.5 embryos where primary fiber cell extension is minimal in the homozygous mutant.

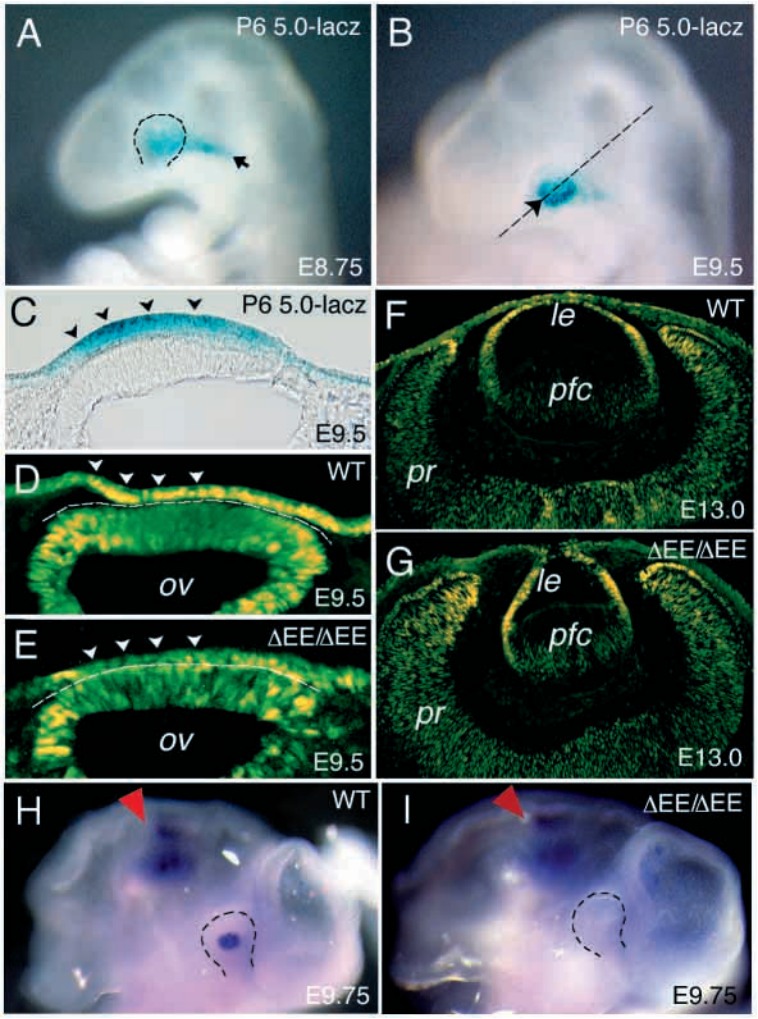

Fig. 5. *Pax6* and *Foxe3* expression in *Pax6*$^{\Delta EE/\Delta EE}$ mice. (A-C) *P6 5.0-lacz* reporter animals stained with X-gal. (A) At E8.75 X-gal staining appears in a teardrop-shaped region of surface ectoderm that overlies the optic vesicle (broken line) and extends temporally (arrow). (B) By E9.5 expression is most intense in a crescent-shaped region that corresponds to the nasoventral lens placode. The broken line indicates the section plane used for C-E and the arrowhead the intense X-gal staining on the nasal side of the lens placode. (C) Frozen section from an X-gal stained E9.5 *P6 5.0-lacz* reporter animal showing stronger staining in the nasal region (black arrowheads) of the surface ectoderm overlying the optic vesicle. (D,E) Pax6 immunofluorescence in cryosections of wild-type (D) and *Pax6*$^{\Delta EE/\Delta EE}$ (E) eye primordia at E9.5. The broken white line indicates the border between surface ectoderm and optic vesicle (ov). This analysis indicates that the level of Pax6 immunoreactivity is greatly diminished in *Pax6*$^{\Delta EE/\Delta EE}$ embryos in the nasal ectoderm of the lens placode (compare arrowed region in D with the equivalent region in E). The zone of diminished Pax6 immunoreactivity in *Pax6*$^{\Delta EE/\Delta EE}$ embryos corresponds to the region where X-gal staining is strongest in the *P6 5.0-lacz* reporter (arrowed region in C). (F,G) Pax6 immunofluorescence in cryosections of wild-type (F) and *Pax6*$^{\Delta EE/\Delta EE}$ (G) eyes at E13.0. Wild-type (H) and *Pax6*$^{\Delta EE/\Delta EE}$ (I) E9.5 embryos subject to whole-mount in situ hybridization with an antisense *Foxe3* probe. This indicates that in wild-type embryos, *Foxe3* expression is found in the ectoderm of the lens placode as expected. In homozygous mutant embryos, *Foxe3* expression is lost from the lens placode, but not from the midbrain region (red arrowheads). The optic cup that surrounds the lens pit is marked by a broken line. ov, optic vesicle; le, lens epithelium; pfc, primary fiber cells; pr, presumptive retina.

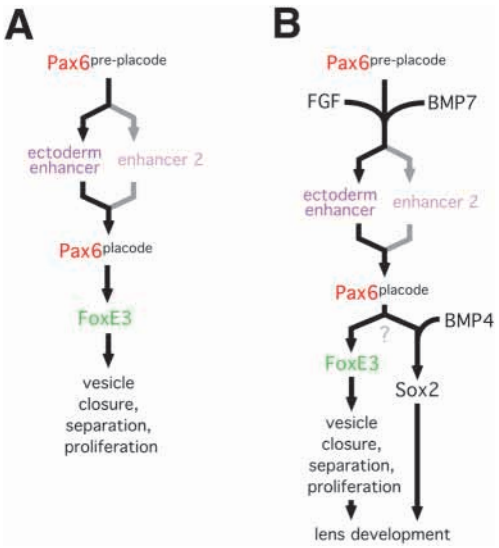

Fig. 6. Proposed models for *Pax6* ectoderm enhancer involvement in lens induction and development. (A) Pathway assembled from the data reported here, and (B) with data incorporated from previous analyses. The black arrows indicate demonstrated genetic interactions, the gray arrows interactions that are implied. The highest component of the proposed pathway is the first phase of *Pax6* expression in the pre-placodal ectoderm (defined as *Pax6*$^{pre\text{-}placode}$). Previous work has shown that *Pax6*$^{pre\text{-}placode}$ is required for the placodal phase of *Pax6* expression (defined as *Pax6*^{placode}). The reduced, but still present, *Pax6* expression observed in *Pax6*$^{\Delta EE/\Delta EE}$ embryos argues for the presence of multiple enhancer elements (denoted as *ectoderm enhancer* and *enhancer 2*) that together confer complete placodal *Pax6* expression. Significantly, reduction of Pax6 protein in the lens placode results in loss of *Foxe3* expression, showing that a threshold level of Pax6 is required for its expression. This indicates that *Foxe3*, a forkhead transcription factor necessary for vesicle closure, separation and proliferation, is genetically downstream of *Pax6*^{placode}. Recent work has shown that Fgf receptor activity and Bmp7 cooperate in maintaining *Pax6*^{placode}, and that *Pax6*^{placode} and Bmp4 within the optic vesicle are required for *Sox2* expression in the lens placode. The genetic relationship between *Foxe3* and *Sox2* remains to be determined.

expression in the lens ectoderm is first observed at E9.5 and continues in the developing and adult lens epithelium (Blixt et al., 2000). To determine whether *Foxe3* expression might be affected by ectoderm enhancer deletion, we performed whole-mount in situ hybridization using a *Foxe3* probe. Wild-type E9.75 embryos show the expected pattern of *Foxe3* expression in both the lens placode and the midbrain (Fig. 5D). In *Pax6*$^{\Delta EE/\Delta EE}$ littermates, the lens placodal expression is undetectable (Fig. 5E), even though the midbrain domain of *Foxe3* expression is retained (Fig. 5E, arrowhead). This indicates

that expression of *Foxe3* in the lens lineage is dependent on wild-type levels of Pax6 and suggests that *Foxe3* lies downstream of *Pax6* in a genetic pathway for lens development.

DISCUSSION

We have investigated the function of the *Pax6* gene in lens induction and development by generating a gene-targeted mouse in which an upstream, ectoderm-specific enhancer (Williams et al., 1998) is deleted. Homozygous mutant mice ($Pax6^{\Delta EE/\Delta EE}$) have distinctive changes in lens formation at all stages. These changes include a lens placode of reduced thickness in the nasal half and a small lens pit and lens vesicle. Even though the maturing lens is smaller in size in these animals, fiber cell differentiation occurs, albeit with some delay. Interestingly, in homozygous mutant mice, the lens vesicle does not separate from the surface ectoderm. Immunodetection of Pax6 in the lens placode of homozygous mutant mice shows that levels are reduced, but primarily in the nasal aspect. In addition, we find that expression of the lens lineage transcription factor *Foxe3* is undetectable. These observations raise several interesting questions concerning the function and regulation of *Pax6* in lens induction, and help to define the genetic pathways required.

Pax6 expression in the lens placode is likely mediated by multiple enhancers

Several experiments have shown that *Pax6* is necessary for lens induction. Tissue recombinations using both wild-type and *Sey/Sey* rat presumptive lens ectoderm and optic vesicle have indicated that *Pax6* expression in surface ectoderm is essential for lens formation (Fujiwara et al., 1994). Similarly, when chimeric mice are generated using wild-type and *Sey/Sey* cells, homozygous mutant cells do not contribute to lens lineage structures (Quinn et al., 1996; Collinson et al., 2000). Finally, conditional gene targeting techniques were used recently to confirm that lens formation does not occur when the placodal phase of *Pax6* expression is eliminated (Ashery-Padan, et al., 2000).

Previous work has also shown that the *Pax6* upstream ectoderm enhancer can direct gene expression in the lens lineage beginning at E8.75 (Williams et al., 1998). When combined with the knowledge that *Pax6* is required for lens development, we might have predicted that deletion of this control element would result in an absence of *Pax6* expression and as a consequence, an absence of lens formation. Interestingly however, Pax6 protein was still detectable and lens development occurred in the $Pax6^{\Delta EE/\Delta EE}$ mice, even though there were distinctive defects at every step.

The most likely explanation is that the upstream ectoderm enhancer does not act alone in permitting *Pax6* expression in the lens placode. Many different transcriptional control elements have been identified in *Pax6* (Kammandel et al., 1999; Xu et al., 1999; Lauderdale et al., 2000), but to date, only the one deleted in this study (Williams et al., 1998) is known to be active in the lens lineage. We can predict that a second element (or combination of elements) active in ectodermal derivatives should be identifiable. Thus, in a genetic pathway describing lens development (Fig. 6A), we include two distinct enhancers that are proposed to combine to give a complete pattern and level of *Pax6* expression in the placode. In the future, it will be very interesting to determine how different enhancer input signals might be combined.

Distinct *Pax6* expression subdomains exist in the lens placode

Examination of the progression of EE-driven expression from E8.75 to E9.5 demonstrates that the *Pax6* ectoderm enhancer mediates *Pax6* expression first over a wide area of the surface ectoderm and then subsequently, in a primarily nasoventral region of the developing lens placode.

Deletion of the upstream ectoderm enhancer in $Pax6^{\Delta EE/\Delta EE}$ mice has led to a graded change in Pax6 levels across the lens placode. The levels of Pax6 immunoreactivity were decreased throughout the placode, with the greatest reduction occurring on the nasal side. From this we can conclude that there are different subdomains of *Pax6* expression within the lens placode and that distinct enhancers mediate expression within these subdomains. Thus, the *Pax6* EE appears primarily responsible for controlling *Pax6* expression in the nasoventral aspect of the lens placode. The combined results of the gain-of-function experiment (the *P6 5.0-lacz* reporter animals), together with the loss-of-function experiment (the $Pax6^{\Delta EE/\Delta EE}$ mice) showing a reciprocal gain and loss of expression on the nasal side of the lens placode strongly support the case for the placodal subdomains we have defined. Based on the phenotype of the $Pax6^{\Delta EE/\Delta EE}$ mice, we can further suggest that evolution of the ectoderm enhancer was an adaptation to increase the size of the lens and to allow the formation of a lens that was separated from the surface ectoderm and therefore distinct from more primitive eye types where the lens and cornea form a single fused 'refractosome' (Duke-Elder, 1958; Piatigorsky, 2000).

The novel notion that there are subdomains within the lens placode is reinforced by the observation that the reduction in ectodermal thickness in this region is not uniform. Specifically, there is a decrease in placodal thickness primarily in the nasal half. The observation that this corresponds with the nasal domain of the placode in which *Pax6* is preferentially expressed by the EE, and where Pax6 levels are most dramatically reduced suggests a causative link. As placodal thickening is the first overt sign of lens formation, this observation indicates that placodal expression of *Pax6* is important for initiating the cell shape changes that preempt placodal invagination and formation of the lens pit. It will be very interesting to investigate the possibility that placodal subdomains might reflect spatially distinct lens induction stimuli. As the presumptive retina is likely to provide induction signals for lens formation, it is notable that this tissue also displays nasotemporal subdomains. For example, the forkhead family members *BF1* and *BF2* are expressed in the nasal and temporal retina, respectively (Tao and Lai, 1992; Hatini et al., 1994; Dirksen and Jamrich, 1995). It is possible that this type of gene expression pattern might reflect signal exchange during the lens and retina induction phase.

Lens development is highly sensitive to Pax-6 dosage

Histological analysis of $Pax6^{+/\Delta EE}$ and $Pax6^{\Delta EE/\Delta EE}$ embryos supports previous findings that eye development is exquisitely sensitive to Pax6 levels (Schedl et al., 1996; Altmann et al., 1997; Chow et al., 1999; van Raamsdonk and Tilghman, 2000). The notion that Pax6 level is critical for appropriate lens development is illustrated clearly by the intermediate

phenotype observed in heterozygote enhancer deletion embryos. In agreement, we detected lower overall levels of Pax6 in the ectoderm of *Pax6*$^{\Delta EE/\Delta EE}$ embryos compared with wild-type. Thus, the removal of the ectoderm enhancer results in a reduction of Pax6 in the lens anlagen. It is clear from these results that accumulation of a crucial threshold of Pax6 is necessary for the appropriate progression of lens development.

The presence of a Peters' anomaly-like change in *Pax6*$^{\Delta EE/\Delta EE}$ animals is not surprising given previous observation of this defect in some mice and humans heterozygous for *Pax6*-coding region mutations (Hanson et al., 1994). However, it has been reported that in the majority of Peters' anomaly cases, the *Pax6*-coding region is normal (Churchill and Booth, 1996). Our findings introduce the possibility that some Peters' anomaly cases may be due to mutations within the *Pax6* upstream ectoderm enhancer.

Measurement of the proliferative index in the lens placode of E9.5 *Pax6*$^{\Delta EE/\Delta EE}$ embryos showed a significant decrease compared with wild-type. This contrasts with a recent analysis of proliferation in the *Pax6*$^{+/Sey\text{-}1Neu}$ mouse (van Raamsdonk and Tilghman, 2000). This discrepancy is most likely due to the different techniques used to assess proliferation. van Raamsdonk and Tilghman used an anti-phospho-histone H3 antibody to detect mitoses. Labeling by this technique is rare, and the absolute number of events counted correspondingly low. This results in an assay that is relatively insensitive and therefore able to detect only large differences. By contrast, the much higher number of events counted with the BrdU labeling technique results in an assay that is more sensitive and able to detect subtle differences.

The reduced levels of proliferation we observe can presumably explain the smaller size of the lens pit, the lens vesicle and maturing lens. In combination with the observation that Pax6 levels are lower in many placodal cells, we can suggest that in these mutant animals, there may be a smaller population of placodal cells that have attained the wild-type level of Pax6. Interestingly, the reduced level of proliferation in the early lens does not have drastic effects on later lens development. Indeed, as the *Pax6*$^{\Delta EE/\Delta EE}$ animals get older, the relative difference in size between wild-type and homozygous mutant lenses is diminished. From this we can suggest that the most critical role of the *Pax6* upstream ectoderm enhancer is in early lens development. Consistent with this idea is the observation that, as assessed with various crystallin markers, there are only minor delays in lens lineage differentiation in *Pax6*$^{\Delta EE/\Delta EE}$ embryos. This does not translate into a continuing defect in fiber cell differentiation and may simply reflect diminished supply of differentiation-competent epithelial cells due to a lower proliferation rate.

Foxe3 is downstream of placodal *Pax6* expression

The *dysgenetic lens* (*dyl*) mouse has defects in lens vesicle closure and separation, as well as a reduction in proliferation of lens lineage cells. These defects are caused by a null mutation in the gene encoding the forkhead family transcription factor Foxe3 (Blixt et al., 2000; Brownell et al., 2000). Because similar, albeit milder, defects are also observed in *Pax6*$^{\Delta EE/\Delta EE}$ animals, we decided to investigate the expression of *Foxe3*. Interestingly, the moderate and regional decrease in Pax6 protein levels in the lens placode of *Pax6*$^{\Delta EE/\Delta EE}$ mice leads to an undetectable level of *Foxe3* expression. These data suggest that a threshold amount of Pax6 protein is necessary, whether direct or indirect, for appropriate activation of *Foxe3*. Although it has been shown that *Foxe3* expression is lost in the *Pax6*$^{Sey/Sey}$ mouse (Blixt et al., 2000; Brownell et al., 2000), the current analysis allows us to be more precise and to suggest that *Foxe3* expression is dependent upon the placodal phase of *Pax6*. The difference in severity of phenotypes between the *Pax6*$^{\Delta EE/\Delta EE}$ and *Foxe3*$^{dyl/dyl}$ mutant embryos may be due to the distinct genetic backgrounds (and modifier genes) or a residual level of *Foxe3* expression in the *Pax6*$^{\Delta EE/\Delta EE}$ mice that ameliorates the consequences.

Thus, with the data presented here and elsewhere, we can assemble a pathway that describes the genetic relationships between various elements of the lens induction pathway (Fig. 6A). It has be shown previously that there are two phases of *Pax6* expression within the lens lineage (Grindley et al., 1995), and that *Pax6* is first expressed in the head ectoderm (defined (Wawersik et al., 1999) as *Pax6*$^{pre\text{-}placode}$). The later, placodal phase of *Pax6* expression (defined as *Pax6*^{placode}) is dependent on *Pax6*$^{pre\text{-}placode}$ (Grindley et al., 1995); thus, we can define two steps in a genetic pathway describing lens development. With the present analysis, we can suggest that *Pax6*^{placode} is dependent upon the activity of at least two transcriptional enhancers (Fig. 6A) and that sufficient *Pax6*^{placode} is required for appropriate progression through the lens development pathway, despite the presence of normal *Pax6* expression at the earlier phase (*Pax6*$^{pre\text{-}placode}$). In addition, the undetectable level of *Foxe3* expression in the placode of *Pax6*$^{\Delta EE/\Delta EE}$ mice makes a clear statement that *Foxe3* lies downstream of *Pax6*^{placode} (Fig. 6A). The similar phenotype of *Pax6*$^{\Delta EE/\Delta EE}$ and *dyl* mice is consistent with a role for *Foxe3* in regulating proliferation within the lens lineage as well as lens vesicle separation.

Numerous other factors contribute to lens induction and development, and based on various analyses, can be included in a genetic pathway describing the process. Bone-morphogenetic protein-7 (Bmp7) has an important role in eye development (Dudley et al., 1995; Wawersik et al., 1999) and *Bmp7* null animals exhibit a variable phenotype that ranges from anophthalmia to micro-ophthalmia (Dudley et al., 1995). Bmp7 is required for development of the lens placode and in particular, for the expression of *Pax6*^{placode} and for expression of the lens induction marker *Sox2* (Kamachi et al., 1998; Wawersik et al., 1999). Thus, *Bmp7* is understood to participate in lens development in a position between *Pax6*$^{pre\text{-}placode}$ and *Pax6*^{placode} (Fig. 6B). Similarly, it has recently been shown that Fgf receptor activity is required for a full level of placodal *Pax6* expression and that Fgf receptor and Bmp7 signaling cooperate (Faber et al., 2001) (Fig. 6B). Consistent with this proposal is the observation that *Foxe3* expression is down-regulated in embryos where Fgf receptor and Bmp7 signaling in the lens placode has been inhibited. Similarly, Bmp4 activity is required for lens development. In the *Bmp4* null mice, while *Pax6* expression is unaffected, the normal upregulation of *Sox2* in the ocular tissues does not occur (Furuta and Hogan, 1998). This argues that *Bmp4* input to lens development pathways lies between *Pax6*^{placode} and *Sox2*. Thus, with new information derived from the current report, we can propose a more comprehensive genetic pathway (Fig. 6B) that describes the process of lens induction and development.

We thank Alex Joyner for good advice on gene-targeting strategies, for providing the targeting vector PKS*loxP*NT and transgenic *Cre* recombinase animals. We also thank Anna Auerbach and Cathy Guo

for performing the blastocyst injections, Milan Jamrich for providing the *Foxe3* probe, Sam Zigler for anti-crystallin antibodies and Asma Norris for technical assistance.

REFERENCES

Altmann, C. R., Chow, R. L., Lang, R. A. and Hemmati-Brivanlou, A. (1997). Lens induction by Pax-6 in Xenopus laevis. *Dev. Biol.* **185**, 119-123.

Ashery-Padan, R., Marquardt, T., Zhou, X. and Gruss, P. (2000). Pax6 activity in the lens primordium is required for lens formation and for correct placement of a single retina in the eye. *Genes Dev.* **14**, 2701-2711.

Bickmore, W. A. and Hastie, N. D. (1989). Aniridia, Wilms' tumor and human chromosome 11. *Ophthalmic Paediatr. Genet.* **10**, 229-248.

Blixt, A., Mahlapuu, M., Aitola, M., Pelto-Huikko, M., Enerback, S. and Carlsson, P. (2000). A forkhead gene, FoxE3, is essential for lens epithelial proliferation and closure of the lens vesicle. *Genes Dev.* **14**, 245-254.

Brownell, I., Dirksen, M. and Jamrich, M. (2000). Forkhead Foxe3 maps to the dysgenetic lens locus and is critical in lens development and differentiation. *Genesis* **27**, 81-93.

Chow, R. L., Altmann, C. R., Lang, R. A. and Hemmati-Brivanlou, A. (1999). Pax6 induces ectopic eyes in a vertebrate. *Development* **126**, 4213-4222.

Churchill, A. and Booth, A. (1996). Genetics of aniridia and anterior segment dysgenesis. *Br. J. Ophthalmol.* **80**, 669-673.

Collinson, J. M., Hill, R. E. and West, J. D. (2000). Different roles for Pax6 in the optic vesicle and facial epithelium mediate early morphogenesis of the murine eye. *Development* **127**, 945-956.

Cvekl, A. and Piatigorsky, J. (1996). Lens development and crystallin gene expression: many roles for Pax-6. *BioEssays* **18**, 621-630.

Cvekl, A., Kashanchi, F., Sax, C. M., Brady, J. N. and Piatigorsky, J. (1995a). Transcriptional regulation of the mouse alpha A-crystallin gene: activation dependent on a cyclic AMP-responsive element (DE1/CRE) and a Pax-6-binding site. *Mol. Cell. Biol.* **15**, 653-660.

Cvekl, A., Sax, C. M., Li, X., McDermott, J. B. and Piatigorsky, J. (1995b). Pax-6 and lens-specific transcription of the chicken delta 1-crystallin gene. *Proc. Natl. Acad. Sci. USA* **92**, 4681-4685.

Czerny, T., Halder, G., Kloter, U., Souabni, A., Gehring, W. J. and Busslinger, M. (1999). twin of eyeless, a second Pax-6 gene of Drosophila, acts upstream of eyeless in the control of eye development. *Mol. Cell* **3**, 297-307.

Dirksen, M. L. and Jamrich, M. (1995). Differential expression of fork head genes during early Xenopus and zebrafish development. *Dev. Genet.* **17**, 107-116.

Dudley, A. T., Lyons, K. M. and Robertson, E. J. (1995). A requirement for bone morphogenetic protein-7 during development of the mammalian kidney and eye. *Genes Dev.* **9**, 2795-2807.

Duke-Elder, S. (1958). *System of Ophthalmology, Vol. I: The Eye in Evolution.* St Louis, MO: C. V. Mosby.

Faber, S. C., Dimanlig, P., Makarenkova, H. P., Shirke, S., Ko, K. and Lang, R. A. (2001). FGF receptor signalling plays a role in lens induction. *Development* **128**, 4425-4438.

Fujiwara, M., Uchida, T., Osumi-Yamashita, N. and Eto, K. (1994). Uchida rat (rSey): a new mutant rat with craniofacial abnormalities resembling those of the mouse Sey mutant. *Differentiation* **57**, 31-38.

Furuta, Y. and Hogan, B. L. M. (1998). BMP4 is essential for lens induction in the mouse embryo. *Genes Dev.* **12**, 3764-3775.

Grindley, J. C., Davidson, D. R. and Hill, R. E. (1995). The role of Pax-6 in eye and nasal development. *Development* **121**, 1433-1442.

Halder, G., Callaerts, P. and Gehring, W. J. (1995). Induction of ectopic eyes by targeted expression of the eyeless gene in Drosophila. *Science* **267**, 1788-1792.

Hanks, M., Wurst, W., Anson-Cartwright, L., Auerbach, A. B. and Joyner, A. L. (1995). Rescue of the En-1 mutant phenotype by replacement of En-1 with En-2. *Science* **269**, 679-682.

Hanson, I. M., Fletcher, J. M., Jordan, T., Brown, A., Taylor, D., Adams, R. J., Punnett, H. H. and van Heyningen, V. (1994). Mutations at the PAX6 locus are found in heterogeneous anterior segment malformations including Peters' anomaly. *Nat. Genet.* **6**, 168-173.

Hatini, V., Tao, W. and Lai, E. (1994). Expression of winged helix genes, BF-1 and BF-2, define adjacent domains within the developing forebrain and retina. *J. Neurobiol.* **25**, 1293-1309.

Hill, R. E., Favor, J., Hogan, B. L., Ton, C. C., Saunders, G. F., Hanson, I. M., Prosser, J., Jordan, T., Hastie, N. D. and van Heyningen, V. (1991). Mouse small eye results from mutations in a paired-like homeobox-containing gene. *Nature* **354**, 522-525.

Hogan, B. L., Horsburgh, G., Cohen, J., Hetherington, C. M., Fisher, G. and Lyon, M. F. (1986). Small eyes (Sey): a homozygous lethal mutation on chromosome 2 which affects the differentiation of both lens and nasal placodes in the mouse. *J. Embryol. Exp. Morphol.* **97**, 95-110.

Joyner, A. L. I., ed. (1995). Gene targeting: a practical approach. In *The Practical Approach Series* (ed. B. D. H. D. Rickwood), pp. 234. New York: IRL Press at Oxford University Press.

Kamachi, Y., Uchikawa, M., Collignon, J., Lovell-Badge, R. and Kondoh, H. (1998). Involvement of Sox1, 2 and 3 in the early and subsequent molecular events of lens induction. *Development* **125**, 2521-2532.

Kammandel, B., Chowdhury, K., Stoykova, A., Aparicio, S., Brenner, S. and Gruss, P. (1999). Distinct cis-essential modules direct the time-space pattern of the Pax6 gene activity. *Dev. Biol.* **205**, 79-97.

Lauderdale, J. D., Wilensky, J. S., Oliver, E. R., Walton, D. S. and Glaser, T. (2000). 3′ deletions cause aniridia by preventing PAX6 gene expression. *Proc. Natl. Acad. Sci. USA* **97**, 13755-13759.

Makarenkova, H. P., Ito, M., Venkatesh, G., Faber, S. C., Sun, L., McMahon, G., Overbeek, P. A. and Lang, R. A. (2000). FGF10 is an inducer and Pax6 a competence factor for lacrimal gland development. *Development* **127**, 2563-2572.

McAvoy, J. W. (1978). Cell division, cell elongation and distribution of alpha-, beta- and gamma-crystallins in the rat lens. *J. Embryol. Exp. Morphol.* **44**, 149-165.

Nieto, M. A., Patel, K. and Wilkinson, D. G. (1996). In situ hybridization analysis of chick embryos in whole mount and tissue sections. *Methods Cell Biol.* **51**, 219-235.

Peters, A. (1906). Uber angeboren Defektbildung der Descemetschen Membran. *Klin. Mbl. Augenheilk* **44**, 27-40.

Piatigorsky, J. (2000). Review: a case for corneal crystallins. *J. Ocul. Pharmacol. Ther.* **16**, 173-180.

Quinn, J. C., West, J. D. and Hill, R. E. (1996). Multiple functions for Pax6 in mouse eye and nasal development. *Genes Dev.* **10**, 435-46.

Quiring, R., Walldorf, U., Kloter, U. and Gehring, W. J. (1994). Homology of the eyeless gene of Drosophila to the Small eye gene in mice and Aniridia in humans. *Science* **265**, 785-789.

Richardson, J., Cvekl, A. and Wistow, G. (1995). Pax-6 is essential for lens-specific expression of zeta-crystallin. *Proc. Natl. Acad. Sci. USA* **92**, 4676-4680.

Schedl, A., Ross, A., Lee, M., Engelkamp, D., Rashbass, P., van Heyningen, V. and Hastie, N. D. (1996). Influence of PAX6 gene dosage on development: overexpression causes severe eye abnormalities. *Cell* **86**, 71-82.

Stone, D. L., Kenyon, K. R., Green, W. R. and Ryan, S. J. (1976). Congenital central corneal leukoma (Peters' anomaly). *Am. J. Ophthalmol.* **81**, 173-193.

Stoykova, A. and Gruss, P. (1994). Roles of Pax-genes in developing and adult brain as suggested by expression patterns. *J. Neurosci.* **14**, 1395-1412.

Takahashi, T., Nowakowski, R. S. and Caviness, V. S. (1993). Cell cycle parameters and and patterns of nuclear movement in the neocortical proliferative zone of the fetal mouse. *J. Neurosci.* **13**, 820-833.

Tao, W. and Lai, E. (1992). Telencephalon-restricted expression of BF-1, a new member of the HNF- 3/fork head gene family, in the developing rat brain. *Neuron* **8**, 957-966.

Ton, C. C., Hirvonen, H., Miwa, H., Weil, M. M., Monaghan, P., Jordan, T., van Heyningen, V., Hastie, N. D., Meijers-Heijboer, H., Drechsler, M. et al. (1991). Positional cloning and characterization of a paired box- and homeobox- containing gene from the aniridia region. *Cell* **67**, 1059-1074.

van Raamsdonk, C. D. and Tilghman, S. M. (2000). Dosage requirement and allelic expression of PAX6 during lens placode formation. *Development* **127**, 5439-5448.

Walther, C. and Gruss, P. (1991). Pax-6, a murine paired box gene, is expressed in the developing CNS. *Development* **113**, 1435-1449.

Wawersik, S., Purcell, P., Rauchman, M., Dudley, A. T., Robertson, E. J. and Maas, R. (1999). BMP7 acts in murine lens placode development. *Dev. Biol.* **207**, 176-188.

Williams, S. C., Altmann, C. R., Chow, R. L., Hemmati-Brivanlou, A. and Lang, R. A. (1998). A highly conserved lens transcriptional control element from the Pax-6 gene. *Mech. Dev.* **73**, 225-229.

Xu, P. X., Zhang, X., Heaney, S., Yoon, A., Michelson, A. M. and Maas, R. L. (1999). Regulation of Pax6 expression is conserved between mice and flies. *Development* **126**, 383-395.

Zigler, J. S. and Sidbury, J. B., Jr (1976). A comparative study of beta-crystallin from six mammals. *Comp. Biochem. Physiol. B* **53**, 349-355.